論文 / 著書情報
Article / Book Information

Title	Optical and Thermal Properties of Organo-silica/Polyimide Nano-hybrids Derived from Polysiloxazane Copolymers
Authors	Daisuke YORIFUJI, Akiko MATSUMURA, Tomoko AOKI, Yuji TASHIRO, Shigeki KUROKI, Shinji ANDO
Citation	Journal of Photopolymer Science and Technology, Vol. 22, No. 4, pp. 447-454
Pub. date	2009, 6

Journal of Photopolymer Science and Technology
Volume 22, Number 4 (2009) 447-454 ©2009CPST

Optical and Thermal Properties of Organo-silica/Polyimide Nano-hybrids Derived from Polysiloxazane Copolymers

Daisuke YORIFUJI[1], Akiko MATSUMURA[1], Tomoko AOKI[2], Yuji TASHIRO[2], Shigeki KUROKI[1] and Shinji ANDO[1]*

[1]*Department of Chemistry and Materials Science, Tokyo Institute of Technology, 2-12-1 O-okayama, Meguro-ku, Tokyo 152-8552, Japan*
[2]*AZ Electronic Materials (Japan) K.K., Chihama 3300, Kakegawa, Shizuoka, 437-1412, Japan*

A new series of organo-silica/polyimide (PI) nano-hybrid materials were prepared by thermal imidization of blended precursors derived from poly (amic acid) (PAA) and polysiloxazane copolymers (DEN). 4,4'-(Hexafluoroisopropylidene) diphthalic dianhydride (6FDA) and 4,4'-diaminodiphenyl ether (ODA) were used to synthesize the PAA of a fully aromatic fluorinated PI (6FDA-ODA), and 1,2:3,4-cyclobutanetetracarboxylic dianhydride (CBDA) and ODA were chosen to prepare the PAA of semi-aromatic PI (CBDA-ODA). Compared with the traditional silica/PI hybrids prepared from sol-gel method, the novel organo-silica/PI nano-hybrids significantly improved the compatibility between PI and DEN components. The FT-IR spectra of the nano-hybrid films showed that Si–O–Si stretching peaks increased as the increase of DEN content. DEN/6FDA-ODA films exhibited higher transparency than the pristine PI, whereas DEN/CBDA-ODA films were slightly opaque due to the poor compatibility between the phenyl rings of DEN and the alicyclic CBDA structure. All the phenomena caused by the organo-silica nano-hybridization, including the slight decrease in refractive indices, the significant decrease in birefringence, and the variations in thermal diffusivity are explainable by the increase of Si–O–Si linkages which form three-dimensional cross-link networks. The DEN/PI nano-hybrids with high silica contents are promising for electronic and optical applications.

Keyword: polyimide, organo-silica, nano-hybrid, transparency, refractive index

1. Introduction

Polyimides (PIs) are widely known to possess excellent physical and chemical properties such as thermal stability, mechanical strength, resistance to organic solvents, and good processability. Recently, optically transparent PIs with high thermal stability and low refractive index are of great importance in opto-electronic devices, including optical fibers, waveguides, and anti-reflective coatings [1]. Fluorinated PIs, especially trifluoromethyl ($-CF_3$)-containing PIs, and alicyclic PIs have been developed for this purpose [2, 3]. In the current advanced micro-electronic applications, further enhancement in the optical and thermal properties of PI films is strongly expected.

Over the last decade, inorganic/organic nano-hybrid materials have been extensively studied because they can endow possibilities of combining superior properties of different materials [4]. Within the nano-hybrid materials that have been reported, silica (SiO_2)/PI hybrid has attracted considerable attention because silica exhibits high thermal stability, low thermal expansion, and low refractive index [5]. However, most of the reports have been focusing on the mechanical and thermal properties [6-10], and only few studies have turned to such inorganic/polymer hybrid materials to control the optical properties of

Received March 30, 2009
Accepted May 1, 2009

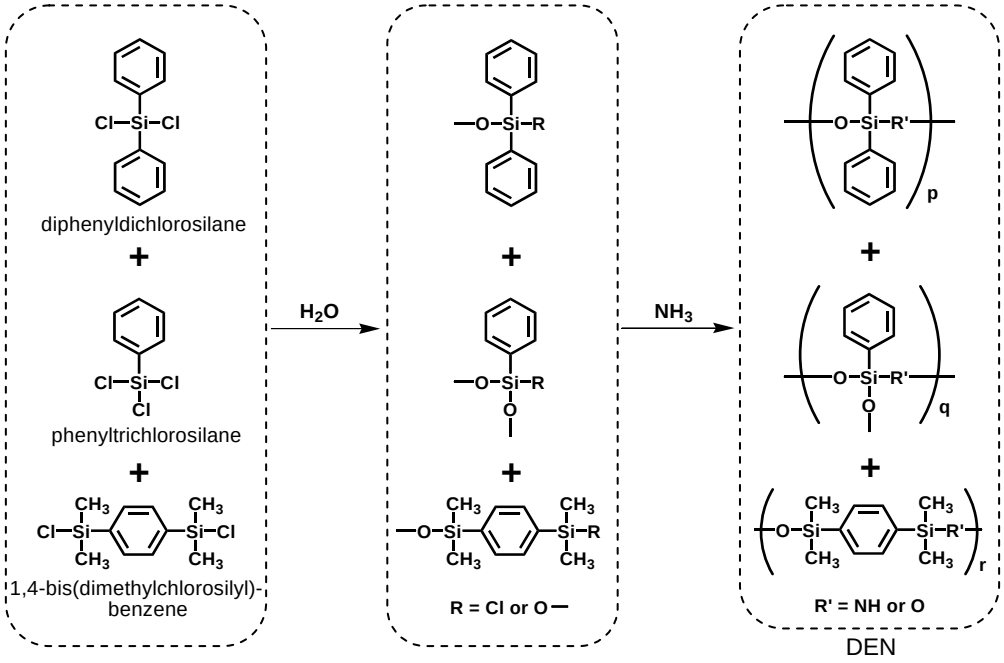

Fig. 1 Reaction scheme and chemical structures of polysiloxazane copolymers (DEN).

the resulting hybrid films.

The traditional sol-gel method for preparation of silica/PI hybrid materials consists of the following procedures: (1) hydrolysis of silica precursor such as tetraethoxysilane (TEOS) to produce silane hydroxide and (2) subsequent formation of three-dimensional network of SiO_2 by polycondensation. The silica/PI hybrid films prepared by the sol-gel method were reported to become opaque with the increase of silica content because of the strong light scattering due to the poor compatibility between silica and PI [11, 12]. This is partially because the size of silica particle increases rapidly with the increase of the silica content in the silica/PI hybrids via the sol-gel method. Use of coupling agent led to more homogeneous silica/PI hybrid films [13-18] as compared to those prepared from PI and TEOS, but the films were still opaque with the increase of silica content [16-18]. Moreover, the thermal stability was slightly deteriorated by the addition of coupling agent [19].

In this study, a new series of organo-silica/PI nano-hybrid films were prepared by the thermal imidization of blended precursors derived from poly (amic acid) (PAA) and polysiloxazane copolymers. Polysiloxazane copolymers (DEN) were used as the sources of organo-silica to overcome the above problems of sol-gel method as shown in Fig. 1. DEN was expected to improve the compatibility of organo-silica to PIs because of the existence of plural phenyl rings in DEN structure. We used two types of PI: one is 6FDA-ODA as fully aromatic fluorinated PI, and the other is CBDA-ODA as semi-aromatic PI including alicyclic structure as shown in Fig. 2. The chemical structures of the DEN/PI nano-hybrid films were characterized and their optical and thermal properties were extensively investigated by comparison with those of the pristine PIs.

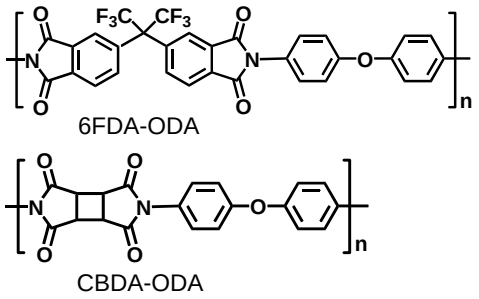

Fig. 2 Chemical structures of polyimides (PIs).

2.Experimental

2.1. Materials

4,4'-(Hexafluoroisopropylidene) diphthalic dianhydride (6FDA) obtained from AZ Electronic Materials (Japan) K.K. was purified by sublimation under reduced pressure before use. 1,2:3,4-Cyclobutanetetracarboxylic dianhydride (CBDA) obtained from JSR corporation was dried at 120°C under reduced pressure. *N*,*N*-Dimethylacetoamide (DMAc, anhydrous, 99.8%) purchased from Aldrich was dried with molecular sieve prior to use. 4,4'-Diaminodiphenyl ether (ODA) purchased from Wako Pure Chemical Industries, Ltd. was

recrystallized from tetrahydrofuran and then sublimated at 180°C under reduced pressure. Diphenyldichlorosilane and phenyltrichlorosilane obtained from Tokyo Chemical Industry Co., Ltd. was directly used as received. 1,4-Bis(dimethylchlorosilyl)benzene obtained from Shin-Etsu Chemical Co., Ltd. was directly used as received.

2.2. Preparation of Polysiloxazane Copolymers

Diphenyldichlorosilane (47.0 g, 0.220 mol), phenyl- trichlorosilane (28.0 g, 0.111 mol) and 1,4-bis(di-methylchlorosilyl)benzene (11.6 g, 0.0444 mol) were dissolved in *m*-xylene in a 2 L there-necked flask fitted with a nitrogen inlet, a thermometer, and a mechanical stirrer. The apparatus was purged with nitrogen gas. The mixture of deionized water (6.8 g, 0.377 mol) and pyridine (1 L) was dripped in the above solution over 20 min at 5°C. Then, the hydrolysis of chlorosilane reaction was further conducted for 1 h at –2°C. After that, ammonia gas was flowed in the reaction mixture at 2 *l* /min for 20 min to react with the unreacted chlorosilane. The successive polycondensation scheme is shown in Fig. 1. At last, the mixed solvent was substituted by *m*-xylene with the solid concentration of 20 wt%, and transparent polysiloxazane blend copolymers (DEN) were thus obtained. The molecular weight (M_w) of DEN determined by GPC was 5,200 g/mol.

2.3. Organo-silica/PI Nano-hybrid Films

6FDA-ODA PAA was prepared by reacting equimolar amounts of 6FDA and ODA in DMAc under nitrogen in ice bath. The setup for reactions was same as that descried for CBDA-ODA PAA (molecular structures are shown in Fig. 2). The solid concentration was fixed to 15 wt%. A transparent PAA solution was obtained after the solution was kept stirring for 8 h.

DEN/PAA precursor solutions were prepared by blending DEN (after solvent substitution) and PAA solutions. A homogeneous precursor solution was thus obtained after stirring for 48 h at room temperature. DEN/PI hybrid films were prepared through spin-coating of solution onto Si substrates, followed by drying at 70ºC for 1 h and thermal imidization at 350ºC for DEN/6FDA-ODA and at 300ºC for DEN/CBDA-ODA for 1.5 h under nitrogen flow. A schematic diagram of the processes is shown in Fig. 3. The preparation procedures for DEN/PI hybrid films is shown in Table 1. We call hereafter DEN/6FDA-ODA and DEN/CBDA-ODA as ‘6F series’ and ‘CB series’, respectively. The thicknesses of the hybrid films were 14–20 μm.

2.4. Measurements

Infrared absorption spectra (IR) were obtained with a Thermo-Nicolet AVATAR-320 FT-IR spectrometer. Solid state ^{29}Si cross polarization / magic angle spinning (CP/MAS) NMR spectra were measured with a Bruker DSX-300 spectrometer operating at the resonance frequencies of 59.6 MHz for ^{29}Si. The sample rotor was spun at a rate of 16 kHz, and the repetition time and the contact time for polarization transfer were set to 5 s and 2 ms, respectively. ^{29}Si chemical shifts were calibrated indirectly through

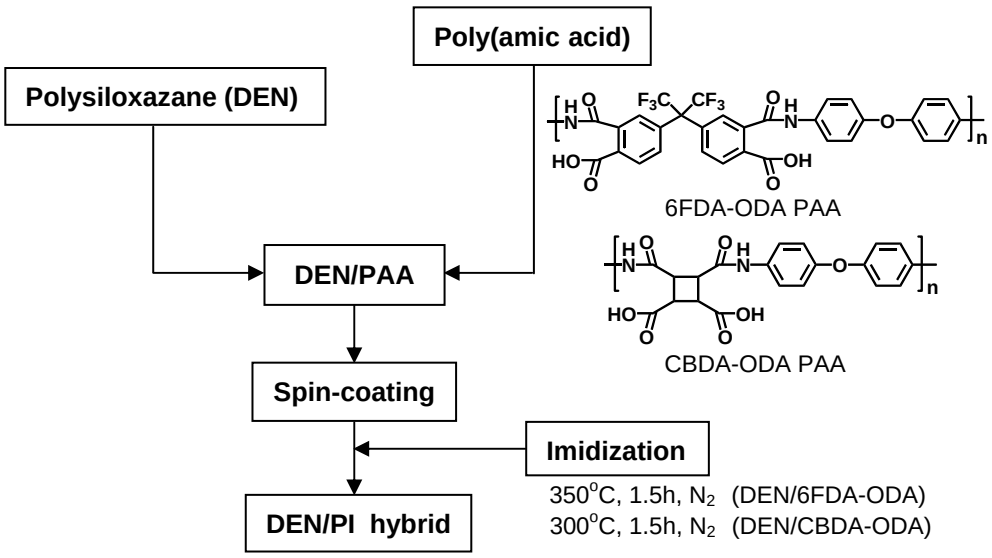

Fig. 3 Preparation flow chart of DEN/PI hybrid.

Table 1 Chemical components and thermal properties of DEN/PI hybrid films.

Sample	Weight ratio		DEN content	T_g	T_d^5	CTE	$a_\perp$
	PI	DEN	(wt%)	(°C)	(°C)	(ppm/°C)	(x 10^{-8} m^2/s)
6F-0	100	0	0	284	506	59.4	12.1
6F-20	100	20	16.7	285	473	65.9	9.7
6F-40	100	40	28.6	285	475	68.4	10.5
6F-60	100	60	37.5	285	479	76.4	11.0
CB-0	100	0	0	330	438	49.9	12.8
CB-20	100	20	16.7	332	438	58.8	7.6
CB-40	100	40	28.6	333	441	60.2	8.7
CB-60	100	60	37.5	334	443	66.8	11.1

the signal of poly(dimethyl siloxane) (–33.6 ppm from TMS). ^{29}Si magnetic shielding calculations of the model structures of DEN (Table 3) were performed using the DFT theory with the B3LYP functional and the 6-311G+(2d,p) basis set. ^{29}Si chemical shifts of the model structures were calibrated by the calculated magnetic shielding of TMS. GAUSSIAN package (Ver. 03, Rev. D.02 or later) [20] was used for the quantum chemical calculations.

UV-vis absorption spectra of the films were acquired with Hitachi U-3500 spectrophotometer. Refractive indices were measured using a prism coupler (Metricon, model PC-2010) at 1324 nm for the in-plane (n_{TE}) and out-of-plane (n_{TM}) polarizations. The in-plane / out-of-plane birefringence (Δn) was calculated as the difference between n_{TE} and n_{TM}. The average refractive index was calculated according to the equation: $n_{av} = [(2n_{TE}^2+n_{TM}^2)/3]^{1/2}$.

Thermal stabilities of the hybrid films were performed with a Shimadzu TGA-50 analyzer in the temperature range from room temp. up to 900ºC at a heating rate of 10ºC/min under nitrogen. The coefficient of thermal expansion (CTE) of the hybrid films (20 mm long and 4 mm wide) was measured by Seiko TMA/SS6100 over the temperature range of 50°C to 250 °C with a heating rate of 5 °C/min. Glass transition temperatures (T_g) were measured by Seiko DSC/SS6100. Thermal diffusivity along the out-of-plane direction ($a_\perp$) was measured with a temperature wave analyser (ai-Phase Mobile 1u) [21].

3. Results and Discussion

3.1. Characterization of DEN/PI hybrid Films

Fig. 4 illustrates the FT-IR spectra of the hybrid films of (a) 6F series and (b) CB series prepared with different amounts of DEN. The intensities of the peaks were normalized at 1724 cm^{-1} (C=O

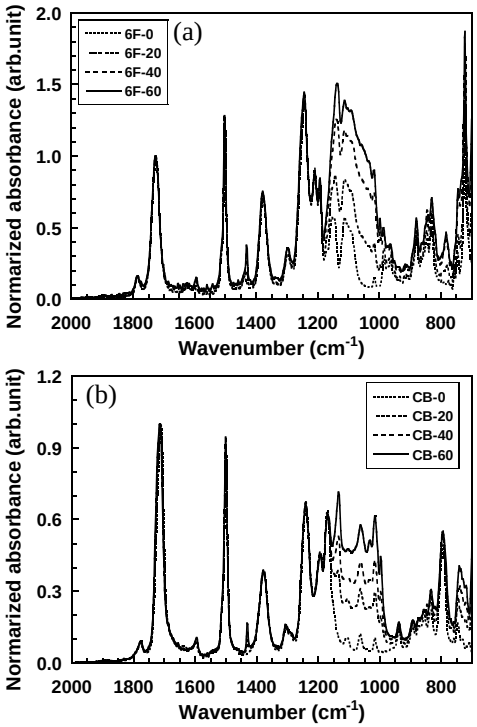

Fig. 4 FT-IR spectra of DEN/PI hybrid films: (a) DEN/6FDA-ODA and (b) DEN/CBDA-ODA. Peak intensities are normalized at 1724 cm^{-1}.

symmetrical stretching of PIs). The broad Si–O–Si band around 1000~1100 cm^{-1} was gradually increased with increasing the DEN content, which confirms the successful hydrolysis and polycondensation reactions of DEN [19].

Fig. 5 shows the solid-state ^{29}Si CP/MAS NMR spectra of the hybrid films of (a) 6F-60 and (b) CB-60. ^{29}Si chemical shifts of the hybrid films are given in Table 2. Over the all NMR spectra measured in this study, the line shapes and peak positions were not affected by the amount of DEN, so that only the spectra of 6F-60 and CB-60 are presented. Recently, theoretical calculation is a powerful tool for spectral assignments for ^{1}H and ^{13}C NMR [22]. Hence, an experimental literature

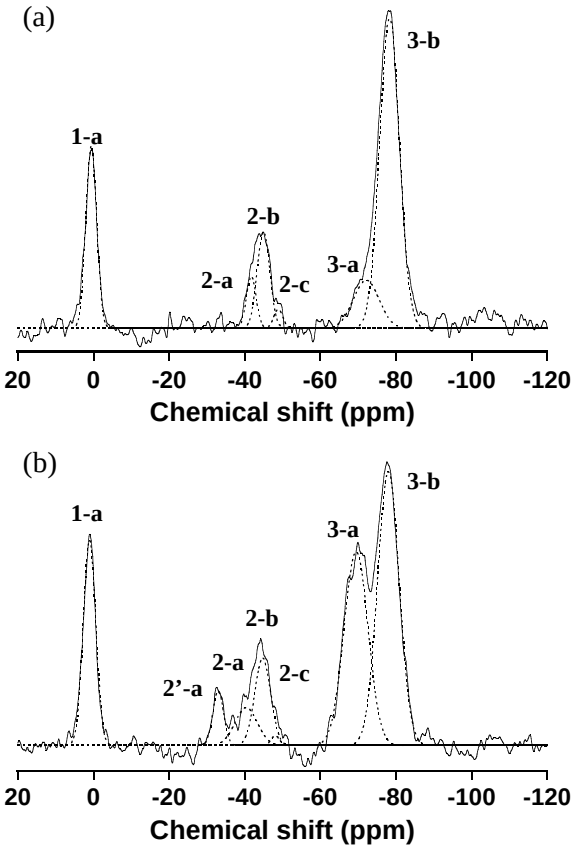

Fig. 5 Solid state ^{29}Si CP/MAS NMR spectra of the hybrid films: (a) 6F-60 and (b) CB-60.

and theoretical calculations were used for peak assignments of ^{29}Si NMR signals. The peak of 3-b was assigned to *T*(ph) (see Table 3) from the experimental results of ^{29}Si NMR by Suzuki et al. [23]. The calculated chemical shifts obtained for model compounds of repeating unit of DEN are summarized in Table 3. For convenience, the following notations were used in this study: '*M* ' (mono-), '*D*' (di-), and '*T* ' (tri-) mean the number of Si–O structures, and 'M_N', 'D_N' and 'T_N' represent the total number of one Si–N and other Si–O structures, respectively. All the terminals of the model compounds were capped by $-Si(CH_3)_3$. The DFT calculations demonstrated that systematic errors of ca. 8 ppm exist between the theoretical and experimental chemical shifts for *T*(ph) structure. By assuming the same tendency for the other functional groups, all the peaks except for 3-a and 3-b were reasonably assigned. The calculated chemical shifts are listed in Table 3, and the spectral assignments are summarized in Table 2.

Table 2 ^{29}Si NMR chemical shifts for hybrid films and the possible structures estimated by calculated chemical shifts.

Peak No.	DEN/6F DA-ODA	DEN/CB DA-ODA	Possible structures
1-a	0.6	1.1	M (ph, $(CH_3)_2$), M_N (ph, $(CH_3)_2$)
2'-a	–	-32.9	D_N (ph_2)
2-a	-41.7	-40.3	D (ph_2) , T_N (ph)
2-b	-44.9	-44.7	D (ph_2) , T_N (ph)
2-c	-48.8	-48.0	D (ph_2) , T_N (ph)
3-a	-72.1	-69.4	T (ph)
3-b	-78.3	-77.9	T (ph)

In comparison between 6F and CB series, two major differences were detected: (1) the peak of 2'-a was observed only for 6F-60, and (2) the ratios of the intensities for 3-a and 3-b peaks were quite different between 6F-60 and CB-60. Such differences could be explained as follows. For 6F series (a), $D_N(ph_2)$ structure derived from diphenyldichlorosilane was not formed because the hydrolysis of chlorosilane to oxysilane was completed, and all diphenyl- dichlorosilane were turned to be $D(ph_2)$ structure during polycondensation. On the other hand, for CB series (b), $D_N(ph_2)$ and $D(ph_2)$ structures were formed during polycondensation, and the adjacent couplings of *T*(ph) and $D_N(ph_2)$ increased the ratio of 3-a peak compared to that of 6F series [24]. Different reaction conditions for DEN precursors during hydrolysis were clearly identified by ^{29}Si CP/MAS NMR spectra.

Table 3 Calculated chemical shifts for model compounds of repeating unit of DEN ($-Si(CH_3)_3$ terminated).

Notation	M_N (ph, $(CH_3)_2$)	M (ph, $(CH_3)_2$)	D_N (ph_2)	D (ph_2)	T_N (ph)	T (ph)
Model compound	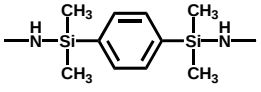	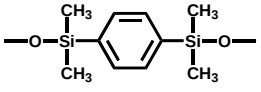	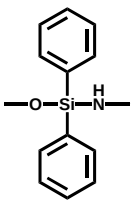	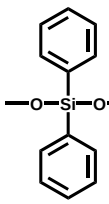	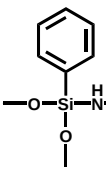	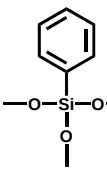
Calculated δ (ppm)	-2.3	-3.4	-35.6	-53.5	-64.0	-86.3

3.2. Optical Properties of DEN/PI Hybrid Films

The refractive indices of the pristine PI and DEN/PI hybrid films are listed in Fig. 6 and Table 4. The pristine 6FDA-ODA PI (6F-0) shows a lower refractive index than CBDA-ODA PI (CB-0). Refractive index (n_{av}) is closely related to density (ρ) and molecular polarizability (α) of repeating unit as follows (Lorentz-Lorenz equation):

$$\frac{n_{av}^2+1}{n_{av}^2+2}=\frac{1}{3\varepsilon_0}\frac{\rho N_A}{M}\alpha$$
$$=\frac{1}{3\varepsilon_0}K_p\frac{\alpha}{V_{vdw}} \quad ,$$

where N_A represents the Avogadro's number, M the molar mass of molecular, and V_{vdw} the van der Waals volume of the repeating unit. α/V_{vdw} stands for the polarizability per volume which directly relates to the degree of electron mobility, and K_p represents the packing coefficient which reflects of the degree of molecular packing.

The lower refractive index of 6F-0, which is due to the smaller α/V_{vdw} and K_p, is attributable to the bulky and low polarizable $-CF_3$ groups. For the both series of 6F and CB hybrids, the refractive indices are decreased by increasing the DEN content, which is attributable to the following factors : (1) the lower refractive index of DEN than those of pristine PIs (Table 4) owing to the three-dimensional Si–O–Si networks with loose molecular packing [25, 26] and (2) the loose molecular packing of PI chains itself resulted from the penetration of DEN into PIs.

In addition, it should be noted that the birefringence (Δn) of the hybrid films, which represents the anisotropy of refractive index, is significantly reduced by nano-hybridization with DEN. This phenomenon could be caused by the introduction of inter-penetrating Si–O–Si networks, which make the hybrid films more isotropic with lower degree of molecular orientation of PIs [18]. In the pristine PIs, 6F-0 also shows a lower birefringence than CB-0, which is due to the sterically crowded and spatially extended structure of 6F-0. From this reason, the reduction of birefringence in 6F series was not as marked as that in CB series.

Fig. 7 shows the UV-visible absorption spectra of the hybrid films. In the pristine PIs, CB-0 shows higher optical transparency than that of 6F-0, which is due to the weaker charge transfer (CT) absorption originated from the lower electron-accepting property of CBDA than that of

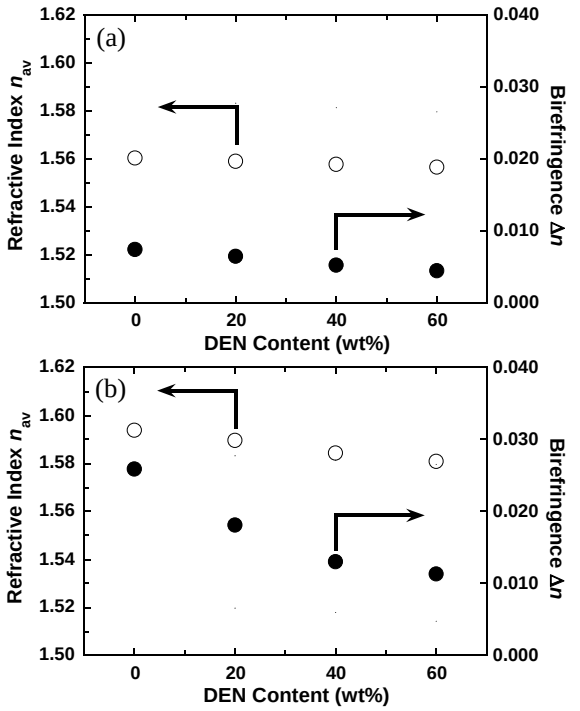

Fig. 6 Refractive indices (n_{av}) (white circles) and birefringence (Δn) (black circles) of DEN/PI hybrid films: (a) DEN/6FDA-ODA and (b) DEN/CBDA-ODA (wavelength: 1324 nm).

6FDA [3]. In the hybrids, 6F series exhibited higher transparency than the pristine PI, whereas CB series became slightly opaque with increasing the DEN content. The light scattering observed in CB series was similar to that of silica/PI hybrid films via the sol-gel method [16–18]. In the sol-gel method, sufficient amounts of chemical bonding between silica and PI chains were formed by dianhydride end-capped PI and coupling agent of silica. The barrier between these two phases is macroscopically blurred by the chemical modification. However, the opaqueness of the DEN/PI hybrid films could be caused by the Mie scattering because the size of silica particles was

Table 4 In-plane, out-of-plane, average refractive indices (n_{TE}, n_{TM}, and n_{av}), and in-plane/out-of-plane birefringence (Δn) observed for DEN/PI hybrid films.

Sample	n_{TE}	n_{TM}	n_{av}	Δn
6F-0	1.5653	1.5575	1.5627	0.0078
6F-20	1.5636	1.5568	1.5613	0.0068
6F-40	1.5626	1.5569	1.5607	0.0057
6F-60	1.5622	1.5572	1.5605	0.0050
CB-0	1.6032	1.5765	1.5943	0.0267
CB-20	1.5930	1.5748	1.5870	0.0182
CB-40	1.5890	1.5725	1.5835	0.0165
CB-60	1.5873	1.5715	1.5820	0.0158
DEN	1.5483	1.5504	1.5490	–0.0022

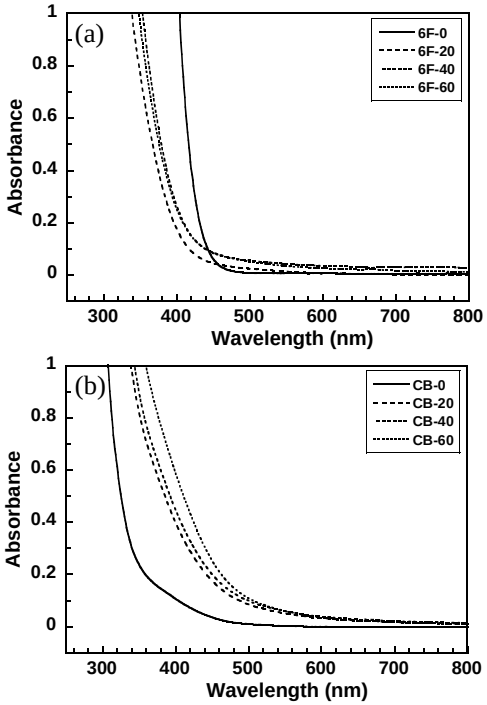

Fig. 7 UV-vis spectra of DEN/PI hybrid films: (a) DEN/6FDA-ODA and (b) DEN/CBDA-ODA.

rapidly increased with increasing the silica content. Thus, the lowered transparency of CB series is explainable by the serious scattering caused by the aggregation of DEN phase. This might originate from the poor compatibility between the phenyl rings of DEN and the alicyclic CBDA structure.

On the other hand, the improved transparency observed for 6F series can be explained by the following factors: (1) significant reduction in the Fresnel refraction at the film surfaces, which was caused by the lowered refractive index, (2) dilution effect based on the loose molecular packing of PI chains, which was caused by penetration of DEN into PI phase, and (3) reduced light scattering caused by the lower aggregation of DEN phase. The last factor is due to the high compatibility between DEN and PI even at high silica contents and the smaller number of chemical bondings between the two phases compared with the silica/PI hybrids via the sol-gel method. The lower aggregation of DEN could be the most essential for the improved transparency of 6F-series.

3.3. Thermal Properties of DEN/PI Hybrid Films

The thermal properties of the DEN/PI hybrid films are summarized in Table 1. In the pristine PIs, 6F-0 exhibited a higher T_d^5 than that of CB-0. On the other hand, the T_d^5s of 6F series were lower than that of the pristine PI (6F-0), whereas the T_d^5s of CB series were increased with increasing the

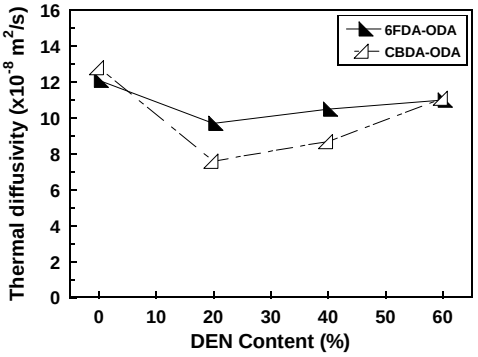

Fig. 8 Thermal diffusivity $a_\perp$ of DEN/PI hybrid films.

DEN content. This suggests that the T_d^5 of DEN exist between those of 6F-0 and CB-0. In contrast, the T_gs of 6F and CB series were unchanged by organo-silica hybridization, which indicates that the introduction of Si–O–Si network does not affect the molecular rigidity of the PI chains.

The CTEs of the hybrid films were increased with increasing the DEN content, which is contrary to the hybrid films prepared by the traditional sol-gel method. Firstly, the chemical bonding between DEN and PI are weaker than those of the silica/PI hybrids via the sol-gel method. Secondly, a robust three-dimensional Si–O–Si network is generally formed by the sol-gel method because silica structures in the hybrids mainly consist of quaternary oxygen tetrahedral ($Si(O_{1/2})_4$). On the other hand, the phenyl groups of DEN would prevent the robust formation of Si–O–Si network in the DEN/PI hybrids [27]. Thus, the increased CTE of DEN/PI hybrid films could be caused by the weak interactions between the two phases and the loosely packed Si–O–Si network.

Fig. 8 shows the thermal diffusivities along the out-of-plane direction ($a_\perp$) of the hybrid films. In the both cases (6F and CB series), the $a_\perp$ values were increased with increasing the DEN content. However, the $a_\perp$ values were decreased from 0 to 20% of DEN content. Based on the phonon conduction theory, heat mainly transfers along the covalent bonds along the molecular chains than the van der Waals bonds across the molecular chains [28]. In general, PI films exhibit low $a_\perp$ values because spin coating process cause significant in-plane orientation of polymer chains in the film plane [29, 30]. Thus, the increase in the isotoropic Si–O–Si network in PI films improved the $a_\perp$ of hybrid films. On the other hand, the decrease in $a_\perp$ from 0 to 20% could be attributed to the loose molecular packing by incorporation of DEN into PI phase. This causes an increase in the surface thermal resistance between PI and DEN. In the

hybrids, the values of $a_{\perp}$ for CB series are lower than those of 6F series, which also suggests that CB series exhibit poor compatibility between DEN and PI than that of 6F series.

4. Conclusion

A new series of organo-silica/polyimide (DEN/PI) nano-hybrid films were prepared by thermal imidization of the corresponding blended precursors which composed of PAA and polysiloxazane copolymers. The chemical structures of DEN component in the hybrids were precisely characterized with FT-IR and solid state ^{29}Si CP/MAS NMR. In contrast to the conventional silica/PI hybrids based on the sol-gel method, DEN/6FDA-ODA hybrid films improved the optical transparency with increasing the DEN content. This is due to the high compatibility between DEN and the fluorinated PI. The hybrid films also exhibited low birefringence and high thermal stability, which are advantageous for the advanced waveguide fabrications. The newly developed DEN/PI nano-hybrid materials with high silica contents are promising for future electronic and optical applications.

References

1. G. O. Shonaike, and S. G. Advani, "*Advanced polymeric Materials"*, CRC press, New York (2003).
2. Q. Li, K. Horie, and R. Yokota, *J. Photopolym. Sci. Technol.*, **10** (1997) 49.
3. S. Ando, *J. Photopolym. Sci. Technol.*, **17**, (2004) 219.
4. G. Kickelbick, "*Hybrid Materials*", Wiley, Weinheim (2007).
5. Y. C. Ke, and P. Stroeve, "*Polymer-layered Silicate and Silica Nanocomposites"*, Elsevier, New York (2005) .
6. C. T. Yen, W. C. Chen, and D. J. Liaw, and H. Y. Lu, *Polymer*, **44** (2003) 7079.
7. S. A. kandary, A. A. M. Ali, and Z. Ahmad, *J. Mater. Sci.*, **41** (2006) 2907.
8. N. Furukawa, M. Yuasa, and Y. kimura, *Polymer*, **40** (1999) 1853.
9. J. W. Huang, Y. L. Wen, C. C. Kang, and M. Y. Yeh, *Polym. J.*, **39** (2007) 654.
10. Z. Shang, C. Lu, X. Lu, and L. Gao, *J. Appl. Polym. Sci.*, **109** (2008) 3477.
11. M. Nandi, J. A. Conklin, L. Salvati, and A. Sen, *Chem. Mater.*, **3** (1991) 201.
12. A. Morikawa, Y. Iyoku, and M. Kakimoto, and Y. Imai, *Polym. J.*, **24** (1992) 107.
13. C. C. Chang, and W. C. Chen, *Chem. Mater.*, **14** (2002) 4242.
14. C. P. Yang, and Y. Y. Su, and S. H. Hsiao, *J. Appl. Polym. Sci.*, **104** (2007) 4046.
15. Y. Li, S. Y. Fu, Y. Q. Li, Q. Y. Pan, G. Xu, and C. Y. Yue, *Compos.Sci.Tec.*, **67** (2007) 2408.
16. Y. Y. Yu, W. C. Chien, and C. L. Lai, *Mat.Chem.Phys.*, **113** (2009) 567.
17. W. C. Liaw, and K. P. Chen, *J. Appl. Polym. Sci.*, **105** (2007) 809.
18. Y. Han, J. Wakita, S. Kuroki, X. Wang, and S. Ando, *J. Photopolym. Sci. Technol.*, **21** (2008) 143.
19. X. Y. Shang, Z. K. Zhu, J. Yin, and X. D. Ma, *Chem. Mater.*, **14** (2002) 71.
20. M. J. Frisch, G. W. Trucks, H. B. Schlegel, G. E. Scuseria, M. A. Robb, J. R. Cheeseman, J. A. Montgomery, Jr., T. Vreven, K. N. Kudin, J. C. Burant, and J. A. Pople, *Gaussian 03, Revision D.02*, Gaussian, Inc., Wallingford CT, (2004).
21. T. Hashimoto, J. Morikawa, T. Kurihara, and T. Tsuji, *Therm. Acta*, **304/305** (1997) 151.
22. H. Tatsuno, and S. Ando, *J. Phys. Chem. B*, **110** (2006) 25751.
23. S. Suzuki, Y. Ono, S. Nakata, and S. Asaoka, *J. Phys. Chem.*, **91** (1987) 1659.
24. G. Engelhardt, and H. Jancke, *J. Organometal. Chem.*, **210** (1981) 295.
25. A. Matsumura, Y.Terui, S. Ando, A. Abe, and T. Takeichi, *J. Photopolym. Sci. Technol.*, **20** (2007) 167.
26. Y. Terui, and S. Ando, *High Perform. Polym.*, **18** (2006) 825.
27. T. Suzuki, Y. Yamada, and K. Itahashi, *J.Appl.Polym.Sci.*, **109** (2008) 813.
28. C. L. Choy, *Polymer*, **18** (1977) 984.
29. Y. Terui, S. Matsuda, and S. Ando, *J. Polym. Sci. Part B*, **43** (2005) 2109.
30. S. Matsuda, and S. Ando, *J. Polym. Sci. Part B*, **41** (2003) 418.